Meccanica (2011) 46: 207–220
DOI 10.1007/s11012-010-9405-x

PARALLEL MANIPULATORS

A novel 3D parallel mechanism for the passive motion simulation of the patella-femur-tibia complex

Nicola Sancisi · Vincenzo Parenti-Castelli

Received: 24 September 2009 / Accepted: 26 November 2010 / Published online: 30 December 2010

Abstract Parallel mechanisms have been exploited for the kinematic modelling of the passive motion, i.e. the motion under virtually unloaded conditions, of the patella-femur-tibia human joint. In particular, a new mechanism is devised in this paper: a 3D model of the patella-femur relative motion is presented which, combined with a previous simplified model of the femur-tibia relative motion, provides a suitable tool for the design of knee prostheses. Although less accurate than a previously presented model of the patella-femur-tibia joint, the new mechanism still replicates passive knee motion quite well and is simpler from a mechanical point of view. Experimental results validate the efficiency of the proposed model.

Keywords Knee model · Patella · Passive motion · Parallel mechanism · Spherical wrist

1 Introduction

Great attention has been devoted to devise kinematic and dynamic models of diarthrodial joints for the scientific as well as technical significance these models have in the orthopaedic and rehabilitation fields. Models make it possible to replicate the joint motion and are a powerful tool on one hand to investigate the role of the main anatomical structures and on the other hand to plan surgical operations and to develop prosthesis design. Moreover, fundamental characteristics such as the joint functionality and stability under various loading conditions may also be efficiently investigated by models.

Kinematic and dynamic models of human joints have been proposed in the literature [3, 7]. Particular attention has been focussed on the human knee joint for the great significance it has in human locomotion. In particular, kinematic knee models for passive motion simulation, i.e. for simulation of motion under virtually unloaded conditions, revealed their importance and effectiveness for a deeper understanding of the role played by the main anatomical structures such as ligaments and articular surfaces in joint motion and stability [5]. They also allow the definition of more feasible boundary conditions for kinetostatic and dynamic models, thus enhancing the performances of these more complex representations of the joint.

A large number of planar models of the knee passive motion have been proposed in the literature, while 3D models have been presented only recently. Consistently with a vast collection of experimental observations, the relative motion of the femur and tibia has been found to be a complex 3D motion with one degree of freedom (DoF), and equivalent spatial parallel mechanisms have been exploited to successfully simulate this motion [10, 11, 13, 14].

N. Sancisi · V. Parenti-Castelli (✉)
DIEM—Department of Mechanical Engineering,
University of Bologna, 40136 Bologna, Italy
e-mail: vincenzo.parenti@unibo.it

Recent investigations show that the relative motion of the patella and femur also has one DoF [1]. However, most models based on equivalent mechanisms do not consider the patella since, based on experimental evidence, it does not play a significant role in the knee passive motion. In contrast, the patella plays a fundamental role both in the motion and in the stability of the tibio-femoral joint when forces are considered in active knee flexion. Therefore modelling the patello-femoral joint is of the utmost importance when equivalent mechanisms are used to define feasible boundary conditions for kinetostatic and dynamic models of the whole knee joint (patella-femur-tibia system).

To the authors' knowledge only one 3D model of the knee joint based on equivalent spatial mechanisms and comprehensive of the patella has been proposed in the literature [12]. This model is basically represented by a parallel mechanism which comprises two main parts. The first part models the relative motion of the tibia and femur by means of a 1-DoF fully parallel mechanism of type 5–5 [11], i.e. a 3D mechanism which features two rigid bodies (representing the femur and tibia) interconnected with five rigid binary links jointed to the rigid bodies by means of spherical pairs. The second part models the relative motion of the patella and femur and it is suitably connected with the first part; in particular, the patella-femur contact is modelled as a hinge. The first part is independent and decoupled from the second one and the whole mechanism has one DoF. The model showed great efficiency in replicating the passive motion of the patella-tibia-femur joint.

In order to devise a knee model which is more suitable to the design of knee prostheses, a simpler model from the mechanical point of view, although less accurate for the motion simulation, was devised for the first part of the whole mechanism [13]. This model is a 1-DoF fully parallel spherical wrist which replaces the 1-DoF 5–5 fully parallel mechanism. With this new mechanism, the tibia-femur relative motion is still replicated with a satisfactory approximation while the equivalent mechanism is drastically simplified. However, the relative motion of the patella and femur, when the spherical wrist is taken as the reference mechanism for the tibia-femur relative motion simulation, has still to be modelled in order to have a complete model of the knee.

This paper aims at completing this deficiency. In particular, the paper presents a new model of the patella-femur relative motion which is compatible with the spherical wrist model of the tibio-femoral relative motion and contributes to form a complete model of the knee passive motion. Finally, a comparison with experimental data shows the efficiency of the proposed model.

2 Model definition

The knee is a joint which allows the relative motion between three bones of the legs, i.e. the femur, tibia and patella. Two sub-joints can be recognized according to the bones that enter into contact with each other during knee flexion: the tibio-femoral joint (TF) allows the relative motion between the femur and tibia, and the patello-femoral joint (PF) allows the relative motion between the patella and femur. These motions are guided in general by articular surfaces (the femur and tibia condyles, the trochlea and the back surface of the patella), by passive structures (such as the ligaments) and by active structures (such as the muscles).

The final objective of passive motion models is to replicate the relative motion of the femur, tibia and patella when no loads are applied to the articulation. The muscles can intrinsically exert forces but, in general, they do not oppose, to any significant degree, external forces when inactive. Since no loads are applied to the joint during passive motion, the muscles remain inactive: they do not guide the passive motion of the knee and, as a consequence, they are not considered in this study. In order to define an equivalent mechanism which can replicate the passive motion of the knee, it is thus fundamental to understand how articular surfaces and passive structures influence both the TF and the PF motion.

The main reason that led other authors to ignore PF in many passive motion models is that the passive motion of TF is independent from that of PF if tibia flexion is imposed. Thus, the two sub-joints of the knee can be analysed separately and, in particular, TF can be modelled without taking PF into consideration. The explanation of this aspect relies on the anatomical constraints between the two sub-joints. The patella slides on the femoral distal surfaces (i.e. the trochlea and the anterior parts of the femur condyles) while it is connected to the tibia through the patellar ligament, and to the femur through the quadriceps, which does not exert any forces on the patella during passive motion. In

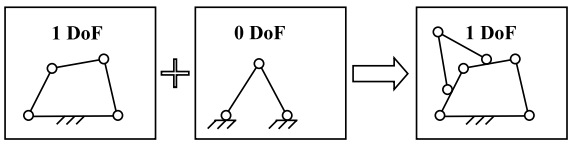

Fig. 1 The two sub-chains of the passive motion model

other words, the patella moves on the femur surfaces being trailed by the patellar ligament.

It is important to note that the independence of the motion of TF from that of PF is also a requirement of the model of the complete joint: the knee model must show the same independence, to make sure it correctly replicates the anatomical constraints of the joint. As a consequence, the equivalent mechanism of the knee passive motion has to be composed of two sub-chains, which fulfill the requirement of partial decoupling. The first sub-chain is the model of TF and, as explained in Sect. 1, it must have one DoF. The second sub-chain is the model of PF: it is connected to the previous one and it must have zero DoFs once the first sub-chain has a given configuration. As a consequence, the complete mechanism exhibits one DoF and the motion of the TF sub-chain is independent from that of the PF sub-chain if knee flexion is imposed. Figure 1 clarifies this concept using a planar mechanism example: the addition of a sub-chain with mobility zero to a mechanism does not change the mobility of the whole mechanism.

The model of the complete joint must show another important feature, in order to be useful for practical application such as surgical planning or prosthetic design. Not only has it to accurately reproduce the relative motion of the femur, tibia and patella in passive conditions, but it also has to be as simple as possible. A simple model allows faster computations and can be identified more easily: this is an important aspect when the model is used for surgical planning or during the operation itself, since the model must adapt quickly to match the anatomical characteristics of the patient. Moreover, a simple mechanism exhibits a low number of members and kinematic pairs (i.e. the number of geometrical parameters which are required to describe the complete structure), a feature which is particularly important for the prosthetic design.

2.1 The tibio-femoral mechanism

The definition of the TF equivalent mechanism is based on anatomical and kinematical considerations

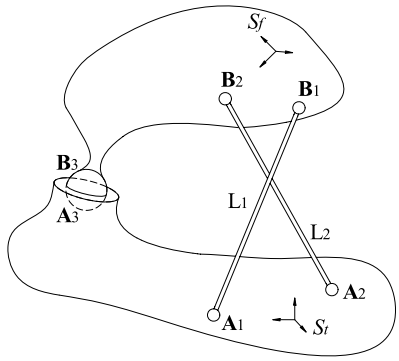

Fig. 2 The 1-Dof parallel spherical wrist

[13]. In particular, it is important to discern which structures of the knee actually influence the TF passive motion: these structures are considered in the model while the others are ignored.

Some studies prove that the instantaneous screw axes of the relative motion between the femur and tibia pass near a particular point [2, 4], as a consequence of the particular shapes of the femoral and tibial condyles. This behaviour is similar to that of two bodies which exhibit a relative spherical motion: all their instantaneous screw axes pass through a point which is the only one that, for a generic displacement, does not move. Other studies prove that a bundle of fibres of the anterior cruciate ligament (ACL) and another one of the posterior cruciate ligament (PCL) remain almost isometric during passive flexion; the other bundles are not tight and reach the limit between laxity and tension at the most [5, 9, 14]. As a consequence, only isometric bundles guide the passive motion of the knee, while the others have no influence on this particular motion and can be ignored in the model.

In conclusion, the relative motion of the femur and tibia in passive conditions is influenced by articular surfaces and isometric bundles. Isometric bundles can be replaced with two rigid links $\mathbf{A}_1\mathbf{B}_1$ and $\mathbf{A}_2\mathbf{B}_2$ (Fig. 2). Each link is connected to the tibia by means of spherical pairs centred at the points $\mathbf{A}_i$ $(i = 1, 2)$ and to the femur by means of spherical pairs centred at the points $\mathbf{B}_i$ $(i = 1, 2)$. Moreover, since the final effect of articular surfaces is to produce a quasi-spherical motion, the condyles can be substituted by a spherical pair which connects the point $\mathbf{A}_3$ on the tibia with the point $\mathbf{B}_3$ on the femur: both $\mathbf{A}_3$ and $\mathbf{B}_3$ are the centre of the spherical pair and thus are the centre of the spherical motion.

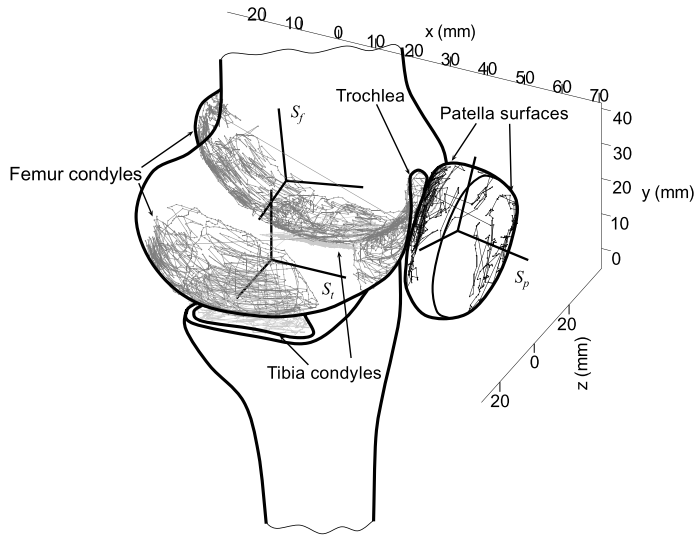

Fig. 3 The three anatomical frames S_t, S_f and S_p represented together with experimental point clouds of the tibial (*light-grey*), femoral (*dark-grey*) and patellar (*black*) articular surfaces

The final TF mechanism is shown in Fig. 2: it features two rigid members (representing the tibia and femur), interconnected with two rigid links (representing the isometric bundles of ACL and PCL) and a spherical pair (representing the centre of the spherical motion). This mechanism is known in the literature as a parallel spherical wrist and it has one DoF, ignoring idle inessential DoFs (i.e. the rotation of links $\mathbf{A}_1\mathbf{B}_1$ and $\mathbf{A}_2\mathbf{B}_2$ about their axis).

If two anatomical frames S_t and S_f are attached respectively to the tibia and the femur, a relative pose (position and orientation) of the femur with respect to the tibia can be expressed by means of the position vector $\mathbf{P}_{tf}$ of the origin of S_f in S_t, and by means of the 3×3 rotation matrix R_{tf} for the transformation of vector components from S_f to S_t. The anatomical frames S_t and S_f are represented in Fig. 3. The tibia anatomical frame is chosen with origin coincident with the tibia centre (on the tibial plateau); x-axis orthogonal to the plane defined by the two malleoli and the tibia centre, anteriorly directed; y-axis directed from the mid-point between the malleoli to the tibia centre; z-axis as a consequence, according to the right hand rule. The femur anatomical frame is defined with origin coincident with the mid-point between the lateral and medial epicondyles; x-axis orthogonal to the plane defined by the two epicondyles and the head of the femur, anteriorly directed; y-axis directed from the origin to the head of the femur; z-axis as a consequence, according to the right hand rule.

Matrix R_{tf} can be expressed as a function of three rotation parameters α, β and γ:

$$R_{tf} = \begin{bmatrix} c_\alpha c_\gamma + s_\alpha s_\beta s_\gamma & -s_\alpha c_\gamma + c_\alpha s_\beta s_\gamma & -c_\beta s_\gamma \\ s_\alpha c_\beta & c_\alpha c_\beta & s_\beta \\ c_\alpha s_\gamma - s_\alpha s_\beta c_\gamma & -s_\alpha s_\gamma - c_\alpha s_\beta c_\gamma & c_\beta c_\gamma \end{bmatrix} \tag{1}$$

where $c_{(\cdot)}$ and $s_{(\cdot)}$ indicate the cosine and sine of the angle $(\cdot)$, and α, β, γ represent the flexion, ab/adduction and intra/extra rotation angles of the femur relatively to the tibia, using a convention deduced by the Grood and Suntay joint coordinate system [6]. According to this convention, flexion is a rotation about the z-axis of S_f, intra/extra is a rotation about the y-axis of S_t, ab/adduction is a rotation about a floating axis, perpendicular to the previous ones. Positive signs of α, β and γ correspond respectively to femoral flexion, adduction and external rotations. Expression (1) can be applied for right legs.

The relative motion of the tibia and femur can be obtained by solving the closure equations of the equivalent mechanism:

$$\begin{aligned} &\left\| \mathbf{A}_i - R_{tf}\mathbf{B}_i - \mathbf{P}_{tf} \right\| = L_i \quad (i = 1, 2) \\ &\mathbf{A}_3 - R_{tf}\mathbf{B}_3 - \mathbf{P}_{tf} = \mathbf{0} \end{aligned} \tag{2}$$

where $L_{1,2}$ are the lengths of the rigid links and the points $\mathbf{A}_{1,2,3}$ and $\mathbf{B}_{1,2,3}$ are the centres of the spherical pairs represented in S_t and S_f respectively. The first two scalar equations constrain $L_{1,2}$ to remain constant, while the last vectorial equation constrains the points $\mathbf{A}_3$ and $\mathbf{B}_3$ to be coincident. If the flexion angle α is assigned, (2) is a system of five equations in the five unknowns β, γ and $\mathbf{P}_{tf}$ components, which can be solved, for instance, by means of a quasi-Newton numerical procedure. The solution defines the relative pose of the femur with respect to the tibia for a given flexion angle.

The coordinates of the points $\mathbf{A}_{1,2,3}$ in S_t, those of the points $\mathbf{B}_{1,2,3}$ in S_f and the link lengths $L_{1,2}$ constitute a set of 20 geometrical parameters which define the TF model. The procedure of identification—based on optimization—is described in Sect. 3.2. The parameters that define the structures which guide the passive motion of TF are thus determined as a result of this preliminary identification procedure.

It is worth noting that the geometry of the TF mechanism can be described by a number of parameters which is actually lower than 20. Four lines $\mathbf{a}_1$, $\mathbf{a}_2$, $\mathbf{b}_1$, $\mathbf{b}_2$ can be defined by connecting the points $\mathbf{A}_1$, $\mathbf{A}_2$ with $\mathbf{A}_3$ and the points $\mathbf{B}_1$, $\mathbf{B}_2$ with $\mathbf{B}_3$. These lines connect the centres of spherical pairs which are fixed with respect to the corresponding reference frame S_t or S_f; as a consequence, lines $\mathbf{a}_i$ are fixed with respect to S_t and lines $\mathbf{b}_i$ are fixed with respect to S_f. Furthermore, four triangles can be defined: $\Delta_{\mathbf{A}_1\mathbf{B}_1}$ with vertices $\mathbf{A}_1$, $\mathbf{B}_1$, $\mathbf{A}_3$; $\Delta_{\mathbf{B}_1\mathbf{B}_2}$ with vertices $\mathbf{B}_1$, $\mathbf{B}_2$, $\mathbf{A}_3$; $\Delta_{\mathbf{A}_2\mathbf{B}_2}$ with vertices $\mathbf{A}_2$, $\mathbf{B}_2$, $\mathbf{A}_3$; $\Delta_{\mathbf{A}_1\mathbf{A}_2}$ with vertices $\mathbf{A}_1$, $\mathbf{A}_2$, $\mathbf{A}_3$ (Fig. 4). Since the mutual distance between the vertices of each triangle is fixed by kinematic constraints, each triangle is a rigid structure which is constrained to rotate about the two axes among $\mathbf{a}_1$, $\mathbf{a}_2$, $\mathbf{b}_1$, $\mathbf{b}_2$ which pass through its vertices. For instance, the triangle $\Delta_{\mathbf{A}_1\mathbf{B}_1}$ is constrained to rotate about the axis $\mathbf{a}_1$ on S_t and the axis $\mathbf{b}_1$ on S_f. Thus, the pairs of spheres on each axis can be substituted by kinematically equivalent hinge joints. As a consequence, the TF model is kinematically equivalent to a spherical four-bar mechanism (Fig. 4).

The spherical four-bar mechanism can be seen as a generalization of the classic knee model which describes the motion of the joint in the sagittal plane by means of a planar four-bar mechanism [8, 9], constituted by two members (representing the tibia and femur) interconnected with two planar rigid links (representing the cruciate ligaments) by revolute pairs. Thus,

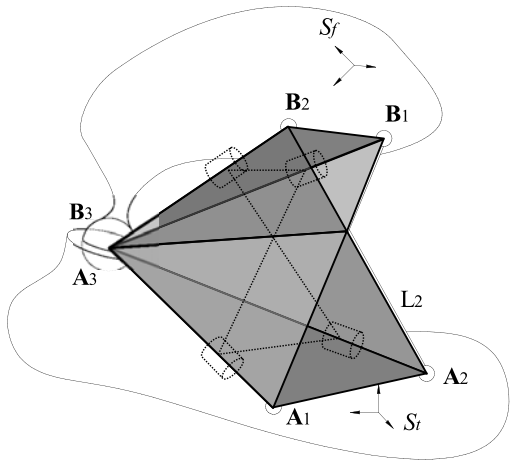

Fig. 4 The kinematic equivalence between the parallel spherical wrist and the spherical four-bar linkage

the number of geometrical parameters required to define the spherical mechanism is 16: the three components of $\mathbf{A}_3$ in S_t, the three components of $\mathbf{B}_3$ in S_f, the eight independent components of the unit vectors of the axis $\mathbf{a}_{1,2}$ and $\mathbf{b}_{1,2}$ in S_t and S_f respectively, the distance L_1 between one arbitrary point on $\mathbf{a}_1$ and another on $\mathbf{b}_1$ and the distance L_2 between one arbitrary point on $\mathbf{a}_2$ and another on $\mathbf{b}_2$.

In other words, 4 out of the 20 parameters which define the geometry of the spherical wrist can be chosen arbitrarily: the points $\mathbf{A}_{1,2}$ and $\mathbf{B}_{1,2}$ can be arbitrarily chosen along the axes $\mathbf{a}_{1,2}$ and $\mathbf{b}_{1,2}$, with no effects on the synthesized relative motion of the tibia and femur. These additional four degrees of freedom in the choice of the geometrical parameters of the equivalent mechanism prove particularly useful for prosthetic design.

2.2 The patello-femoral mechanism

Like the TF model, the equivalent mechanism of PF can be defined by means of anatomical and kinematical considerations about the relative motion of the patella and femur under passive conditions [12]. In order to satisfy the requirement of simplicity for the final model, a characteristic which is fundamental for practical applications, it is important to discern which structures affect the passive motion of the joint also in this case.

The contact between the patella and femur occurs on a wide portion of their rigid articular surfaces for each flexion angle (Fig. 5): this observation

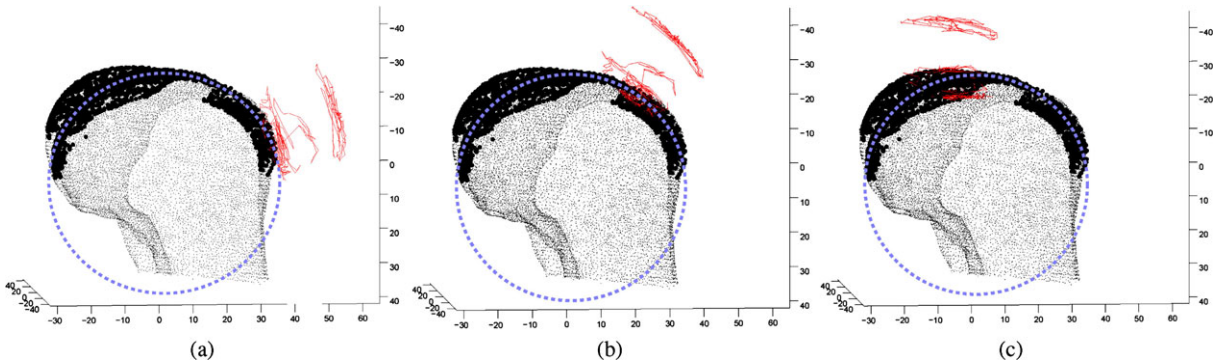

Fig. 5 The articular contacts between the patella (*lines*) and femur (*points*) at three different flexion angles; the cylindrical approximation of the condyles (*dotted circle*) is also presented

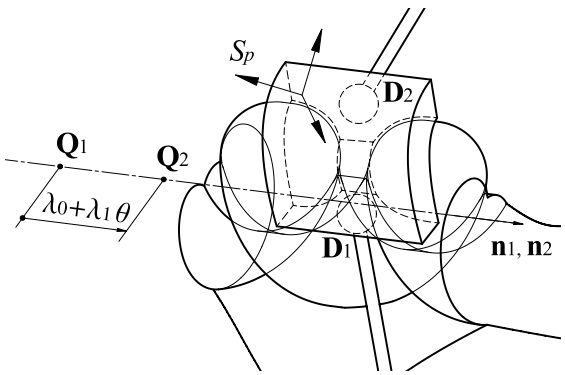

Fig. 6 The kinematic model of the patello-femoral joint; in the figure, the geometrical parameters are also represented

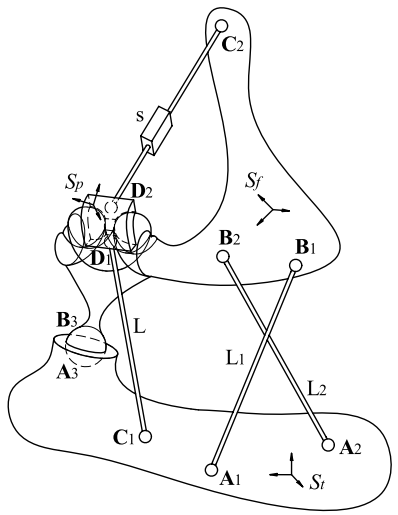

Fig. 7 The kinematic model of the knee joint; in the figure, the geometrical parameters are also represented

suggests that this contact can be modelled by means of a lower pair. In particular, the trochlea and the anterior portions of femoral condyles which are involved in the contact can be approximated by a cylinder. Furthermore, the particular shape of the articular surfaces makes sure that the patella translation along the cylinder axis is guided by articular contacts: the back surface of the patella fits—in a certain sense—the trochlea, the femoral condyles and the intercondylar space which serve as a sort of rail for the patella. This rail almost lays on a plane that, however, is not orthogonal to the cylinder axis: the motion of the patella with respect to the femur is nearly helicoidal. Finally, experimental observations show that a bundle of fibres of the patellar ligament remains almost isometric in passive flexion, while the other bundles are not tight and do not guide the passive motion.

Similarly to TF, the passive motion of PF is thus guided by the isometric bundle of the patellar ligament and by articular contacts. Articular surfaces can be substituted by a screw joint which connects the patella and femur (Fig. 6). The axis of the joint is defined on the femur by the unit vector $\mathbf{n}_1$ and the point $\mathbf{Q}_1$, and on the patella by the unit vector $\mathbf{n}_2$ and the point $\mathbf{Q}_2$. The relative axial position of the patella and femur is defined by parameters λ_0 and λ_1: λ_0 is the distance between $\mathbf{Q}_1$ and $\mathbf{Q}_2$ at a reference position, λ_1 is the axial translation between these two points corresponding to 1 radiant relative rotation of the patella with respect to the femur. Furthermore, the isometric bundle can be substituted by a rigid link of fixed length L, connected to the tibia and patella by means of spherical pairs centred respectively at points $\mathbf{C}_1$ and $\mathbf{D}_1$ (Fig. 7).

Finally, in order to obtain a complete kinematic model of the knee, it is necessary to set the parameter of the motion whose value determines the configuration of the joint. The flexion movement when imposed by the muscles can be seen as the result of the action (lengthening or shortening) of the quadriceps on the patella. In other words, the length of quadriceps fixes the configuration of the joint: this can be accomplished in the model by substituting the quadriceps with a group $\mathbf{C}_2\mathbf{D}_2$ (Fig. 7)—composed of two rigid binary links connected by a prismatic joint—which sets the distance between the centre $\mathbf{D}_2$ of a spherical joint on the patella and the centre $\mathbf{C}_2$ of a spherical joint on the femur, by means of an axial translation parameter s of the prismatic joint. It is worth noting that the quadriceps is actually connected to both the femur and ilium; since the relative motion between the femur and ilium is not considered in this study, these two bones can be seen as a single rigid body.

The model of the whole knee in passive flexion is represented in Fig. 7. It can be obtained by joining the TF and PF equivalent mechanisms. The model has one DoF (ignoring idle inessential DoFs) and the linear displacement s of the prismatic joint defines the configuration of the knee when the flexion angle is imposed by the quadriceps. The PF mechanism indeed is composed of two Assur groups (the first one is composed of the member $\mathbf{C}_1\mathbf{D}_1$ and the patella, the second one is the group $\mathbf{C}_2\mathbf{D}_2$), namely two fixed structures which have mobility zero, if the position of extremity pairs of each group is fixed. In this case, the position of extremity pairs of the two Assur groups is fixed by the TF mechanism. Assur groups do not modify the mobility of the mechanism to which they are connected and, as a consequence, the number of DoFs of the whole knee model is the same as the TF mechanism, i.e. one DoF. This is congruent with the previous anatomical observations: PF does not constrain TF in passive conditions and, if the flexion angle is externally imposed, the motion of TF is independent from that of PF; on the contrary, the motion of PF is defined by the TF model. The movement which is obtained by leaving the prismatic pair idle reproduces the passive motion of the knee.

If an anatomical frame S_p is attached to the patella, the relative pose of the patella with respect to the femur can be expressed by means of the position vector $\mathbf{P}_{fp}$ of the origin of S_p in S_f, and by the 3×3 rotation matrix R_{fp} for the transformation of vector components from S_p to S_f. The anatomical frame S_p is represented in Fig. 3. It is defined with origin coincident with the mid-point between the lateral and medial apices; x-axis orthogonal to the plane defined by the lateral, medial and distal apices, anteriorly directed; y-axis directed from the distal apex to the origin; z-axis as a consequence, according to the right hand rule.

Matrix R_{fp} can be expressed as a function of three rotation parameters α, β and γ, by means of an expression similar to (1). Even though the Grood and Suntay convention was originally defined for the tibio-femoral joint, its application on different joints (the patello-femoral joint included) is becoming common in the scientific literature.

Like the TF model, the relative motion of the patella and femur can be obtained by solving the closure equations of the PF mechanism:

$$\begin{aligned} &R_{fp}\mathbf{n}_2 = \mathbf{n}_1 \\ &R_{fp}\mathbf{Q}_2 + \mathbf{P}_{fp} = (\lambda_0 + \lambda_1\vartheta)\mathbf{n}_1 + \mathbf{Q}_1 \\ &\|R_{tf}(R_{fp}\mathbf{D}_1 + \mathbf{P}_{fp}) + \mathbf{P}_{tf} - \mathbf{C}_1\| = L \end{aligned} \tag{3}$$

where $\mathbf{n}_1$, $\mathbf{Q}_1$ are represented in S_f, $\mathbf{C}_1$ in S_t and $\mathbf{n}_2$, $\mathbf{Q}_2$, $\mathbf{D}_1$ in S_p. The angle ϑ is the rotation of the patella about the screw joint axis with respect to a reference pose. If r_{ij} is an element on the ith row and jth column of the 3×3 rotation matrix for the transformation of vector components from the current to the reference pose of the patella, the angle ϑ can be obtained by:

$$\vartheta = \arcsin\left(\frac{r_{21} - r_{12}}{2n_{2z}}\right) \tag{4}$$

The first two vectorial equations of the system (3) constrain the axis identified by $\mathbf{n}_1$ and $\mathbf{Q}_1$ to be coincident with that identified by $\mathbf{n}_2$ and $\mathbf{Q}_2$. Moreover, the second vectorial equation imposes the distance between $\mathbf{Q}_1$ and $\mathbf{Q}_2$, i.e. the relative axial translation of the patella and femur along the screw joint axis. The last scalar equation ensures that the distance between $\mathbf{C}_1$ and $\mathbf{D}_1$ remains constant.

If R_{tf} and $\mathbf{P}_{tf}$ are known by solving the closure equations (2), the system (3) is composed of seven equations in six unknowns, i.e. the three components of $\mathbf{P}_{fp}$ and the angles α, β, γ which define R_{fp}. However, in the first vectorial expression of (3) only two out of three equations are independent, since $\mathbf{n}_1$ and $\mathbf{n}_2$ both have unitary norms. Thus, once R_{tf} and $\mathbf{P}_{tf}$ are obtained from (2), the system (3) makes it possible to find the relative poses of the patella and femur at each

assigned flexion angle. It is worth noting that if the flexion angle is externally imposed, the PF motion depends on that of TF: this is an anatomical constraint which is satisfied in the model.

The geometrical parameters involved in the PF model (Fig. 6) are the components of the unit vectors $\mathbf{n}_1$ and $\mathbf{n}_2$ of the screw axis represented respectively in S_f and S_p, the coordinates of the points $\mathbf{Q}_1$ and $\mathbf{Q}_2$ represented respectively in S_f and S_p, the coordinates of the points $\mathbf{C}_1$ and $\mathbf{D}_1$ represented respectively in S_t and S_p, the fixed distance L between $\mathbf{C}_1$ and $\mathbf{D}_1$ and the two parameters which define the axial translation λ_0 and λ_1. Since the norms of the unit vectors $\mathbf{n}_1$ and $\mathbf{n}_2$ are unitary, their components can be expressed as a function of four independent coordinates only (two for $\mathbf{n}_1$ and two for $\mathbf{n}_2$ components). Furthermore, since the points $\mathbf{Q}_1$ and $\mathbf{Q}_2$ can be arbitrarily chosen on the screw axis, each of them can also be expressed as a function of two independent coordinates only.

As a consequence, the PF model is described by a set of 17 independent geometrical parameters. The parameters which define the position of points $\mathbf{C}_2$ and $\mathbf{D}_2$ are not taken into account since they are not necessary for the solution of the position analysis problem of the mechanism in passive flexion: since the prismatic joint is idle, the group $\mathbf{C}_2\mathbf{D}_2$ does not influence the motion of either the patella or the femur. The procedure of identification is described in Sect. 3.2; as a result, the structures which guide the passive motion of PF are identified. The set of 16 parameters of the TF sub-chain and the set of 17 parameters of the PF sub-chain define the complete model of the knee under passive loading conditions.

3 Identification of the model

3.1 Experimental session

An experimental session was carried out, in order to collect the experimental data which make it possible to define the model of the knee passive motion, according to the geometrical and kinematical considerations outlined in the previous section. During the same experiment, the relative motion of the femur, tibia and patella was recorded: the experimental motion is used as a reference both in the identification procedure and in the result analysis, to evaluate the accuracy of the proposed model.

A right leg deriving from an amputation was analysed. The leg was declared as normal by the surgeon who assisted during data acquisition. Anatomical landmarks were recorded by means of an opto-electronic system: the anatomical frames S_f, S_t and S_p were thus defined from these preliminary measurements. The same opto-electronic system was used to acquire the relative motion of the femur, tibia and patella under unloaded conditions; in particular, this motion was recorded as a set of 68 relative poses which spanned a flexion arc with range 5–114 degrees. As a result, the matrices R_{tf}, R_{fp} and the position vectors $\mathbf{P}_{tf}$, $\mathbf{P}_{fp}$ were obtained at the 68 flexion angles. For the sake of conciseness, the experimental motion is shown in Figs. 9–12 together with the results of the model.

The knee was then anteriorly cut and the anatomical structures were exposed. The anatomical surfaces were digitized by means of the same tool used to collect the relative motion: the femur and tibia condyles, the trochlea and the front and back surfaces of the patella were thus obtained as clouds of points in the corresponding anatomical frame (Fig. 3). The ACL and PCL attachment areas were digitized similarly. The experimental session was originally focussed on the TF and thus not all data required by the PF model were collected. In particular, the attachment areas of the patellar ligament were not digitized and were thus reconstructed from photographic material.

3.2 Parameter optimization

In order to define a physically relevant model, the topology of the mechanism, its geometry and, as a consequence, its geometrical parameters should stem from experimental observations on the clinical and kinematical characteristics of the joint. This is an important point to relate the simulation results of the model to the experimental ones, an aspect which becomes fundamental when the model is used for the study of the joint, for surgical purposes or for prosthetic design.

All these considerations lead to the choice of optimization as a method for the identification of the model parameters. In particular, bounded optimization procedures make it possible to find the parameter set which reduces to a minimum the errors between the experimental and the simulated motions, at the same time keeping the parameter values sufficiently close to the anatomical observations. Both the

TF and the PF equivalent mechanisms are identified by means of bounded optimization techniques. Starting from a first approximative solution (the first guess) deduced from the anatomical data, the optimum set of $16 + 17$ parameters is obtained which best-fits the experimental motion of the knee. Two distinct optimization problems are solved, namely the identification of the TF mechanism and that of the PF mechanism. The passive motion model could be identified in a single step: the choice of a two step optimization—which is possible thanks to the partial decoupling of the two sub-chains of the mechanism—simplifies the computations. Moreover, since the first approximate solutions are based on the anatomical remarks explained in Sects. 2.1 and 2.2, the optimal solutions have to be sufficiently close to these first guesses. Thus, the parameters of the first approximations are used also as a reference to define the domains of research, i.e. the bounds, for the optimization procedure.

The preliminary geometry of the spherical wrist is obtained from the experimental data. The relative positions of the ACL and PCL attachment areas from total extension to maximal flexion are analysed in passive conditions and for each ligament the pair of points (one on the femur and the other on the tibia) which show the minimal change in distance is chosen. These two pairs of points define the isometric bundles. The two points on the tibia ($\mathbf{A}_1$ and $\mathbf{A}_2$) and those corresponding on the femur ($\mathbf{B}_1$ and $\mathbf{B}_2$) are the centres of the spherical pairs on the two rigid links of the equivalent mechanism. The length L_1 is defined as the distance between the points $\mathbf{A}_1$ and $\mathbf{B}_1$ at full extension; the length L_2 is defined accordingly. Finally, the helical axes of the relative motion between the femur and tibia are computed at each pair of consecutive relative poses; these axes are obtained both on S_t and on S_f. The centre of the spherical wrist on the tibia ($\mathbf{A}_3$) is chosen as the point whose sum of distances from the helical axes on S_t is minimum; the wrist centre on the femur ($\mathbf{B}_3$) is chosen accordingly.

As regards the PF equivalent mechanism, the femoral articular surfaces of PF are approximated by a best-fitting cylinder in S_f: the axis of the cylinder makes it possible to obtain the unit vector $\mathbf{n}_1$ and the point $\mathbf{Q}_1$. The relative pose of the patella and femur corresponding to a flexion angle centred in the considered flexion arc is chosen as the reference pose. The projections of $\mathbf{n}_1$ and of the position vector of $\mathbf{Q}_1$ in S_p at the reference pose allow $\mathbf{n}_2$ and $\mathbf{Q}_2$ to be defined; the distance between $\mathbf{Q}_1$ and $\mathbf{Q}_2$ sets the λ_0 parameter. The λ_1 parameter is obtained, instead, from the angle between $\mathbf{n}_1$ and the perpendicular to the plane which approximately contains the intercondylar space. Finally, the attachment areas of the patellar ligament are analysed: the pair of points (one on the tibia, the other on the patella) which exhibit the minimal change in distance during the experimental movement (isometric bundle) define the points $\mathbf{C}_1$ and $\mathbf{D}_1$; their mean distance sets the L length.

The optimization techniques applied to the TF and PF mechanisms are substantially similar. As regards the spherical wrist, 12 flexion angles are chosen among the 68 experimental ones, as a compromise between the accuracy and the computational time of the procedure and in order to be coherent with previous published results [12]. The 12 flexion angles cover the full flexion arc and are almost equally-spaced: the difference between two consecutive flexion angles is nearly 10 degrees. This difference is not a fixed value, since this was not allowed by the tool used to acquire the experimental poses. At each optimization iteration, the closure equations (2) are solved at the 12 chosen angles. The relative poses of the femur and tibia computed from the model are iteratively compared with the experimental ones: the sum of the weighted squares of errors between the poses constitutes the error index F which has to be minimized. In particular, if x_{ji} is the computed value of the jth unknown ($j = 1, \ldots, 5$) of the system (2), obtained at the ith flexion angle ($i = 1, \ldots, 12$), the contribution of x_{ji} to the value of F is:

$$\epsilon_{ji}^2 = \frac{(x_{ji} - x_{ji}^\star)^2}{x_{jd}^2} \tag{5}$$

where $x_{ji}^\star$ is the corresponding experimental value of the unknown. The weights x_{jd} are necessary, since the unknowns have different physical dimensions (some are angles, others are lengths). The weights only depend on the experimental values of the unknown and are chosen as:

$$x_{jd} = \max\left\{x_{j1}^\star, x_{j2}^\star, \ldots, x_{j12}^\star\right\} - \min\left\{x_{j1}^\star, x_{j2}^\star, \ldots, x_{j12}^\star\right\} \tag{6}$$

Thus, the error ϵ_{ji} is a sort of per cent error, with respect to the maximum range x_{jd} of the jth pose parameter.

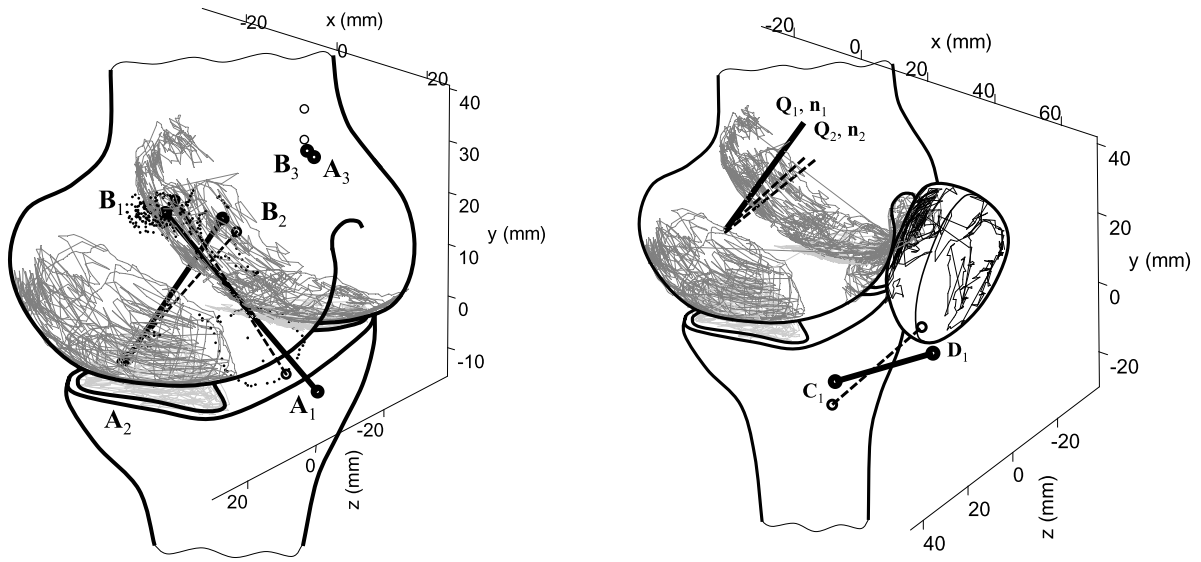

(a) The TF mechanism. (b) The PF mechanism.

Fig. 8 The first estimate (*dashed lines* and *thin circles*) and the optimized (*solid lines* and *thick circles*) models of the TF (**a**) and PF (**b**) sub-joints; the anatomical surfaces and the ligament attachment areas are also included

The mechanism closure is not guaranteed for every parameter set: if the model closures are not satisfied at all the given flexion angles, an arbitrary high value is assigned to the index F. Thus, the complete algorithm for the computation of F is:

$$\begin{aligned} F &= \sum_{j=1}^{5}\sum_{i=1}^{12}\epsilon_{ji}^2 \quad \text{if closure succeeds} \\ F &= X \qquad\qquad\quad \text{otherwise} \end{aligned} \tag{7}$$

where X is an arbitrary high value. As previously noted, in order to give the proposed model a physical consistency, the optimization research domain is bounded, having the first approximative solution as the central value: every parameter q_n $(n = 1, \ldots, 16)$ has to fall within the domain interval $[q_{0n} - \delta_n, q_{0n} + \delta_n]$, where q_{0n} is the first guess and δ_n is a fixed half-length of the interval. Since F is highly non-linear and presents discontinuities, the problem (7) is solved initially by means of a genetic algorithm; this solution is then refined by means of a quasi-Newton algorithm. The solution is the parameter set which minimizes the F error index within the bounds.

As regards the PF equivalent mechanism, the same 12 flexion angles as the TF model are considered, and the corresponding experimental relative poses between the patella and femur are selected. The relative poses of the femur and tibia are obtained from the previously optimized TF model. These simulated poses are used to solve the closure equations (3) of the PF sub-chain at each given flexion angle. The solutions are then compared to the experimental poses of the patella and femur. The optimization procedure and the computation of the F error index are very similar to those used to identify the TF model. It is worth noting, however, that the simplicity of the PF equivalent mechanism makes sure the model closures are satisfied at each considered flexion angle, within the bounds. As a consequence, F is continuous within the bounds and the optimum solution can be searched for by means of quasi-Newton algorithms. Another difference with respect to the TF model is the number of pose parameters which are fitted, i.e. 6 instead of 5: contrary to the TF flexion angles, the patella α rotation is not imposed on the PF mechanism, whose motion is completely defined by the motion of the TF equivalent mechanism.

The results of the identification of the TF and PF mechanisms are reported in Fig. 8. The dashed lines and thin circles represent the first estimate of the parameters of the model, while the solid lines and thick circles are the same parameters after the optimization procedure. In particular, the rigid links $\mathbf{A}_1\mathbf{B}_1$ and $\mathbf{A}_2\mathbf{B}_2$ and the centre of the spherical motion $\mathbf{A}_3$ and $\mathbf{B}_3$

are shown in Fig. 8a; the rigid link $\mathbf{C}_1\mathbf{D}_1$ and the axis of the screw joint (defined by $\mathbf{Q}_1$, $\mathbf{n}_1$ and $\mathbf{Q}_2$, $\mathbf{n}_2$) are shown in Fig. 8b. The optimized model is close to its first estimate: this aspect gives consistency to the kinematical and anatomical assumptions which lead to the definition of the TF and PF equivalent mechanisms.

4 Results

The simple geometry of the new mechanism made it possible to quickly solve the closure equations and the optimization problem: the calculations took just 5 minutes on a standard personal computer with a 3 GHz processor. Apart from its simplicity, the efficiency of the model is a consequence of its stability and of its high mobility, which reduce the problems connected to the non-existence of closure equation solution, and their consequence on continuity of the error index.

The position and orientation components of S_f in S_t are presented in Figs. 9 and 10: the dotted lines are the experimental data, while the solid ones are the results of the model. Similarly, the synthesized motion of S_p in S_f is compared to the experimental one in Figs. 11 and 12.

The mean errors between the experimental and synthesized motions are reported in Table 1; the per cent errors with respect to the maximum range of each pose parameter are also reported in brackets. The absolute and per cent mean errors are reported both relatively to the new mechanism presented in this paper and relatively to the previous one, presented in [12] and briefly described in the Introduction.

Table 1 Absolute and per cent mean errors between experimental and simulated motion, as synthesized by the previous and the new equivalent mechanisms of the whole knee

Mean errors	TF motion	
	Previous mechanism	New mechanism
β (degrees)	0.17 *(6.66%)*	0.23 *(9.11%)*
γ (degrees)	0.48 *(2.22%)*	1.63 *(7.51%)*
x (mm)	0.73 *(5.67%)*	0.85 *(6.64%)*
y (mm)	0.17 *(5.71%)*	0.24 *(7.83%)*
z (mm)	0.32 *(7.77%)*	0.60 *(14.59%)*
Mean errors	PF motion	
	Previous mechanism	New mechanism
α (degrees)	1.64 *(2.33%)*	1.77 *(2.51%)*
β (degrees)	1.18 *(10.50%)*	1.23 *(10.95%)*
γ (degrees)	2.34 *(9.64%)*	1.89 *(7.78%)*
x (mm)	1.86 *(3.74%)*	0.89 *(1.80%)*
y (mm)	0.95 *(3.91%)*	1.13 *(4.69%)*
z (mm)	0.50 *(10.70%)*	0.48 *(10.39%)*

The new simpler model replicates the knee passive motion with a good accuracy, which remains comparable to that of the previous more complex mechanism. The simplification of the model affects the TF motion, which is slightly less accurate but still close to that of the previous TF mechanism. However, the advantages of the simpler TF model (lower mechanical complexity, lower geometrical parameters, lower computational burden, higher numerical stability) counterbalance the lower accuracy, in particular in all those practical (prosthesis and orthosis design, rehabilitation) and theoretical (full body or lower limb models) applications where complexity is a drawback [13]. Moreover, the new PF model—slightly different from that used in the previous mechanism—makes it possible to compensate for the reduced accuracy of the TF sub-chain and to synthesize a PF motion that, for certain parameters, is even better than the previously obtained one.

In conclusion, the proposed knee model proved efficient in replicating the relative motion of the tibia, femur and patella in passive loading conditions. The same mechanism could also be used to predict the loads in the joint when external forces are applied. However, the analysis of the joint forces should be limited to low loads: high loads can lengthen the fibres of isometric ligaments and of the other passive structures of the knee, thus modifying its configuration; the rigid body assumption at the basis of the proposed mechanism could be a strong approximation of reality in this case, making the model less reliable. However, when high forces are applied to the joint, the equivalent mechanism proposed in this study could be used to obtain a feasible boundary condition (or a first step) for the subsequent generalization of the model that, by considering the stiffness of articular structures, reproduces the kinetostatic and dynamic behaviour of the whole knee.

5 Conclusions

A three-dimensional mechanism which can reproduce the passive motion of the knee comprehensive of

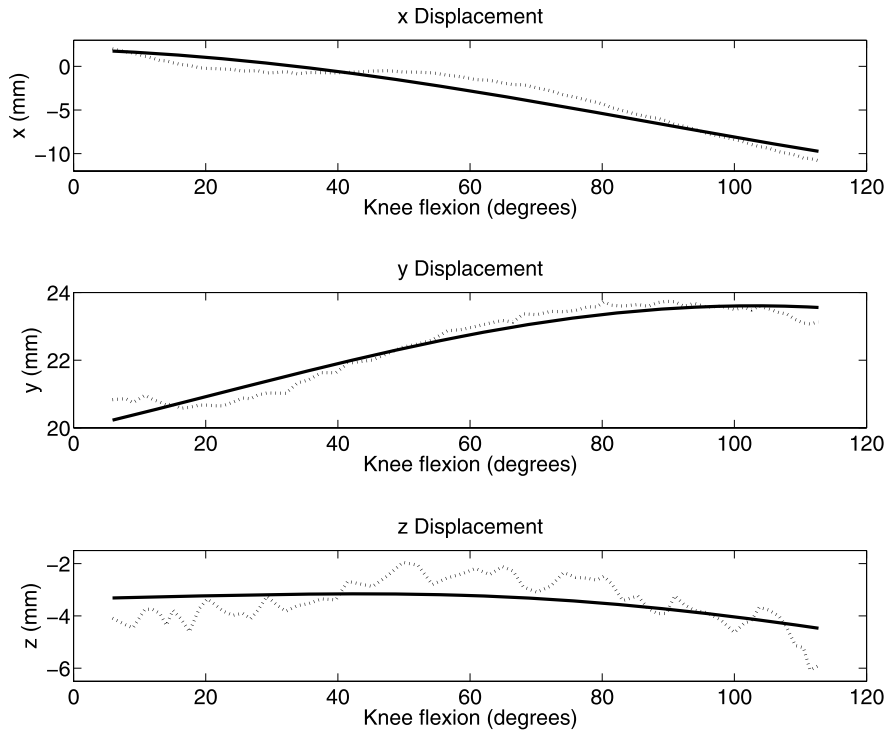

Fig. 9 Position of the origin of S_f with respect to S_t; *dot* = experimental data, *solid* = synthesized motion

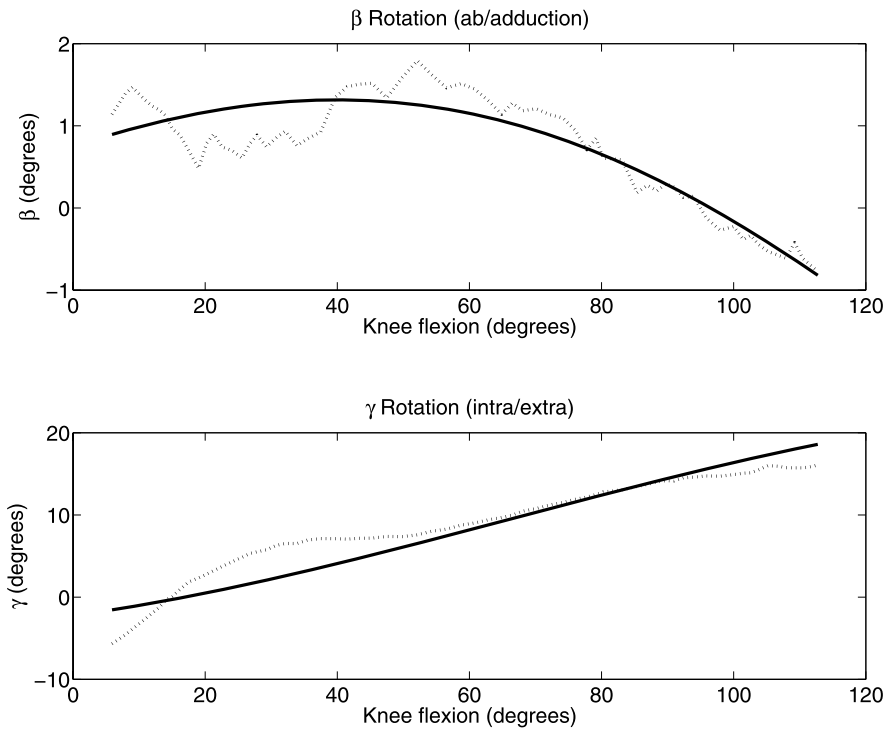

Fig. 10 Orientation of S_f with respect to S_t; *dot* = experimental data, *solid* = synthesized motion

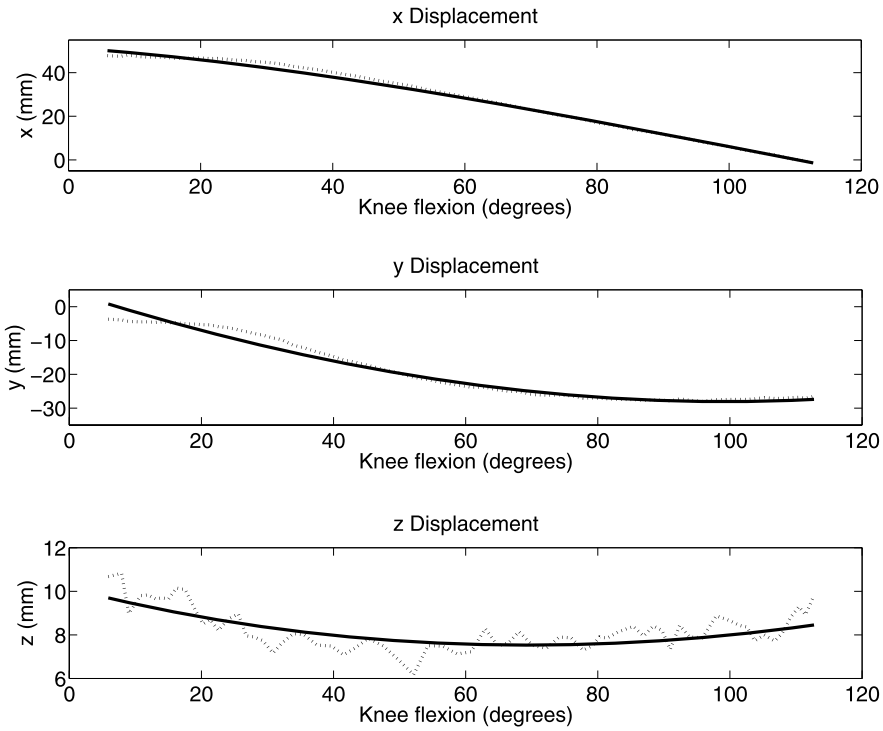

Fig. 11 Position of the origin of S_p with respect to S_f; *dot* = experimental data, *solid* = synthesized motion

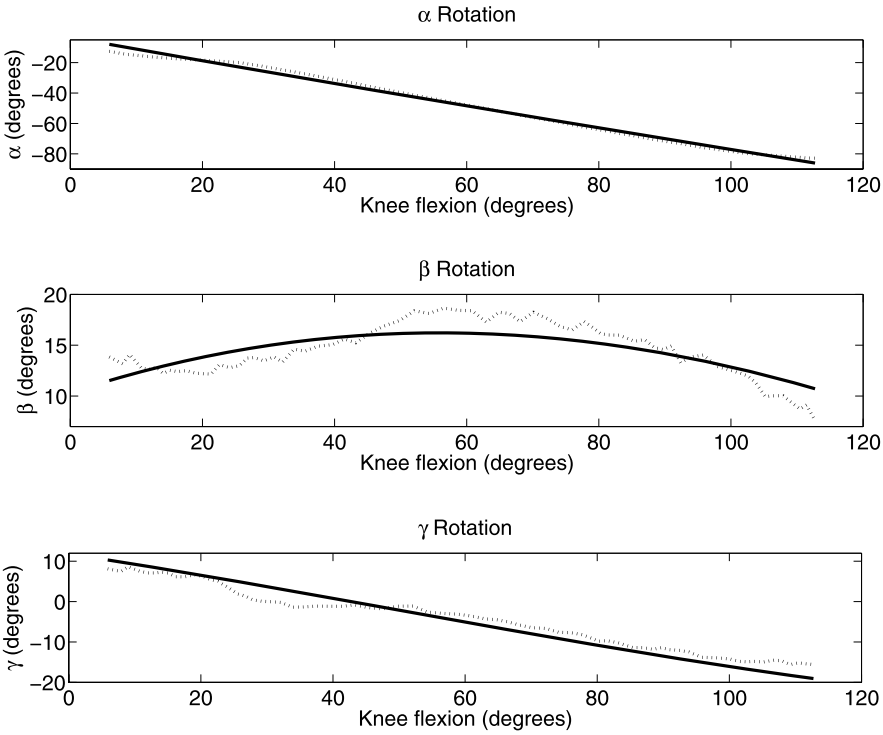

Fig. 12 Orientation of S_p with respect to S_f; *dot* = experimental data, *solid* = synthesized motion

the patella is proposed. The model is defined from anatomical and kinematical considerations and is then identified on experimental data.

The model replicates the passive motion of the tibia, femur and patella with good accuracy. Moreover, its simple geometry makes it particularly useful in practical applications, such as surgical planning or, more specifically, prosthetic design.

Acknowledgements This study was supported by AERTECH-LAB project, funded by Regione Emilia-Romagna, and MIUR funds. The authors wish to thank Dr. Alberto Leardini at Istituto Ortopedico Rizzoli for providing the experimental facilities, Dr. Claudio Belvedere and Dr. Andrea Ensini for their support during experimental sessions.

References

1. Belvedere C, Catani F, Ensini A, Moctezuma de la Barrera JL, Leardini A (2007) Patellar tracking during total knee arthroplasty: an in vitro feasibility study. Knee Surg. Sports Traumatol. Arthrosc. 15(8):985–993
2. Blankevoort L, Huiskes R, Lange AD (1990) Helical axes of passive joint motions. J Biomech 23:1219–1229
3. Erdemir A, McLean S, Herzog W, van den Bogert AJ (2006) Model-based estimation of muscle forces exerted during movements. Clin Biomech 22(2):131–154
4. Fuss FK (1993) Helical axis surface of the knee joint. In: Proceedings of 14th congress of the international society of biomechanics, Paris, France, 4–8 July
5. Goodfellow JW, O'Connor JJ (1978) The mechanics of the knee and prosthesis design. J. Bone Jt. Surg., Br. Vol. 60-B:358–369
6. Grood ES, Suntay WJ (1983) A joint coordinate system for the clinical description of three-dimensional motions: application to the knee. J Biomech Eng 105:136–144
7. Hefzy MS, Cooke TDV (1996) Review of knee models: 1996 update. Appl Mech Rev 49(10–2):187–193
8. Menschik A (1974) Mechanik des Kniegelenks, Teil 1. Z. Orthopädie 112:481–495
9. O'Connor JJ, Shercliff TL, Biden E, Goodfellow JW (1989) The geometry of the knee in the sagittal plane. Proc. Inst. Mech. Eng., H J. Eng. Med. 203(4):223–233
10. Parenti-Castelli V, Leardini A, Di Gregorio R, O'Connor JJ (2004) On the modeling of passive motion of the human knee joint by means of equivalent planar and spatial parallel mechanisms. Auton Robots 16(2):219–232
11. Parenti-Castelli V, Di Gregorio R (2000) Parallel mechanisms applied to the human knee passive motion simulation. In: Lenarcic, J., Stanisic, M. (eds.) Advances in robot kinematics. Kluwer Academic, Dordrecht
12. Sancisi N, Parenti-Castelli V (2007) A new 3d kinematic model of the patello-femoral joint during knee passive motion. In: Proceedings of AIMeTA 2007, Brescia, Italy, 11–14 September, pp 1–12
13. Sancisi N, Parenti-Castelli V (2010) A 1-dof parallel spherical wrist for the modelling of the knee passive motion. Mech Mach Theory 45:658–665
14. Wilson DR, O'Connor JJ (1997) A three-dimensional geometric model of the knee for the study of joint forces in gait. Gait Posture 5:108–115